University of Baghdad
College of Engineering
JE
JOURNAL OF ENGINEERING

Journal of Engineering

journal homepage: www.joe.uobaghdad.edu.iq

Volume 29 Number 3 March 2023

Hydromorphodynamics Simulation for Selected Stretch of Euphrates River within Al-Anbar Governorate

Wasan W. Jaber*
MSc. student
Dept. of Water Resources Engr.
College of Engr..- Univ. of Baghdad
w.al-hadiethy1310@coeng.uobaghdad.edu.iq

Thamer A. Mohammed
Prof., Ph.D.
Dept. of Water Resources Engr.
College of Engr..- Univ. of Baghdad
thamer.a.m@coeng.uobaghdad.edu.iq

ABSTRACT

In this study, the hydromorphodynamic simulation of a stretch of the Euphrates River was conducted. The stretch of the Euphrates River extended from Haditha dam to the city of Heet in Al-Anbar Governorate and it is estimated to be 124.4 km. Samples were taken from 3 sites along the banks of the river stretch using sampling equipment. The samples were taken to the laboratory for grain size analysis where the median size (D_{50}) and sediment load were determined. The hydromorphodynamic simulation was conducted using the NACY 2DH solver of the iRIC model. The model was calibration using the Manning roughness, sediment load, and median particle size and the validation process showed that the error between the simulation and the recorded data was minimum. After calibration, three different scenarios were considered and the scenarios were based on different river discharges (low, average, and flood discharge). Four statistical indices were used to check the predicted values of the velocities and water depth in various sections of the Euphrates River section at the city of Heet and these indices were Mean Absolute Deviation (MAD), Mean Square Error (MSE), Root MSE (RMSE), and the Mean Absolute Percentage Error (MAPE). For velocity values of the above indices for the first scenario were found to be 0.19, 0.046, 0.21, and 0.17 respectively. However, water depth values for the above statistical indices were found to be 0.07, 0.01, 0.01, and 0.13 respectively. The values confirmed the accuracy of the prediction of model iRIC Nacy2DH.

Keywords: Calibration, Euphrates River, hydromorphodynamic, iRIC, simulation

*Corresponding author
Peer review under the responsibility of University of Baghdad.
https://doi.org/10.31026/j.eng.2023.03.09

Article received: 08/08/2022
Article accepted: 20/08/2022
Article published: 01/03/2023

محاكاة عددية لهيدرولوجية ومورفولجية نهر الفرات ضمن محافظة الأنبار

وسن وضاح جابر*
طالبة ماجستير
قسم هندسة الموارد المائية
كلية الهندسة–جامعة بغداد
بغداد– عراق

ثامر احمد محمد
استاذ ، دكتوراه
قسم هندسة الموارد المائية
كلية الهندسة–جامعة بغداد
بغداد– عراق

الخلاصة

في هذه الدراسة, تم انجاز محاكاة هيدروداناميكية لطول محدد من نهر الفرات بطول كلي مقداره 124.4 كم ويمتد من نهاية سد حديثة الى مدينة هيت في محافظة الانبار. اخذت نماذج من ثلاث مواقع مختارة لغرض معرفة نو التربة والحمل الرسوبي لنهر الفرات حيث اخذت النماذج الى المختبرواجريت عليها فحوص التدرج الحبيبي والحمل الرسوبي وبعدها استخدام معدل حجم الحبيبات (D_{50}) في معايرة النموذج العددي. وبعدها تم حساب الخطا في نتائج النموذج علما ان المحاكاة انجزت على سيناريوهات لحالات جريان مختلفة (تصريف واطى وتصريف عالي). تم التحقق من نتائج النموذج الخاصة بالسيناريو الاول باستخدام اربعة مقاييس احصائية وهي معدل الانحراف المطلق, معدل تربيع الخطأ, جذر معدل تربيع الخطأ, ونسبة المعدل المطلق للخطأ. كانت تلك القيم للسرع المتوقعة في مقطع نهر الفرات في مدينة هيت تساوي 0.17 ,0.21 ,0.046 ,0.19 على التوالي. لكن لاعماق النهر ولنفس المقطع كانت هذه القيم الاحصائية هي 0.13 ,0.01 ,0.01 ,0.07 على التوالي. ان قيم المقاييس الاحصائية توكد توكد دقة نتائج نموذج iRIC Nacy2DH.

الكلمات الرئيسية: محاكاة عددية, نهر الفرات, هيدرومورفوديناميك, نموذج iRIC

1. INTRODUCTION

Euphrates River is one of the world's largest overflow rivers, and a substantial portion of it flows through Iraq, transporting massive quantities of sediment. Clay and silt, fine and coarse sands, make up these sediments. The significance of this sand load is that it identifies the downstream sediment budget that is related to channel stability. The silt-clay load contributes to the next region's physical and ecological growth. The discharge amount in that specific region is subject to seasonal conditions. However, the discharge depends on water released from Haditha Dam based on the electricity generation besides demands for various purposes downstream of the Euphrates River **(Kamel, 2008).** Dredging for navigational purposes has thrown a wrench in the next region's budget, **(Attard, 2012).** Annually the river carries thousands of tons of sediments of various kinds, and it is classified into coarse sediments and fine sediments, such as stone, sand, clay, silt, and every type of these sediments has the characteristics that distinguish it from the other type. Flow rate, water depth, and other characteristics are affected by the ability of a river to carry and transport sediments. The bed load in natural river systems remains constant because the same amount of sediment is eroded as it is deposited in a river section. The river receives bed load (e.g., sand or gravel) from upstream catchments and then carried it downstream.

This balance of erosion and deposition can be disrupted by human intervention or natural disasters. Hydraulic structures, in particular, alter the natural flow of a river.
Many studies were conducted on river morphology and hydraulics and selected studies will be reviewed in this study. **(Hiroshi et al., 2011)** experimentally studied the influence of hydraulic structures such as groins and -like structures on morphological processes in natural rivers. Although the usage of such structures are for river banks' protection and the formation of deep navigation channel locally creates complex flow patterns by reducing the flow velocities and also increasing the flood levels. As a result of higher flow velocity behind a hydroelectric power plant or a weir, a higher erosion rate occurred and the sediment is accumulated upstream of the storage structure, resulting in downstream sediment depletion **(Goniva et al., 2012). (Gharbi et al., 2014)** conducted one-dimensional modeling to determine the sediment transport rate, and to visualize the morphological changes in Medjerda River, Tunisia during major floods. In addition, a two-dimensional model for predicting the amounts of materials transported by the river. A comparative analysis was performed between the results of 1D and 2D models including an assessment of benefits and limitations. The results demonstrated that the 2D model can calculate the flow variation, sediment transport rates, and river morphological changes during extreme events for complicated natural domains with high accuracy compared with the 1D Model. **(Mustafa et al., 2016)** included the extraction characteristics of morphological and spatial basins investigated utilizing the Soil and Water Assessment Tools (SWAT) via the (GIS) to discover the quantities of sediments and flow rates flowing into the Haditha reservoir. **(Mingfu and Qiuhua, 2017)** developed a two-dimensional hydro-morphological model which can be used to simulate river hydraulics and morphology with various vegetation covers. The model was validated against many laboratory-scale test cases and then applied to a natural river. **(Hydar et al., 2019)** simulated the hydromorphodynamics of the river's confluence taking the confluence between Kurau and Ara Rivers, in Perak, Malaysia as a case study. The simulation was conducted using a 2D numerical model with the main objective to mitigate the erosion and deposition zones by adopting vanes as control structures. The modeling results suggested the most effective location, dimension, and angle of vanes can be decided based on their performance in scouring and deposition zones. In addition, they concluded that the distribution velocity and flow vectors can help in deciding the location of the vanes. **(Khudair, 2019)** used neural nets (NN) models to study the parameters affecting the transient performance of sewage pump stations which generates unpleasant transportation efficiency. **(Ivan et al., 2022)** investigated the performance of hydraulic conveyance of Ana branching channels as a restoration alternative by assessing the distribution and magnitude of deposition and erosion response patterns. A high-resolution survey indicated aggradation has not occurred within the main channel.
This work is used the hydrological and topographic features of the Euphrates River, which runs for 124.4 kilometers from Haditha Dam to Heet Station and passes through several towns to calibrate and validate a two-dimensional model to predict the hydromorphodynamics of the Euphrates river at the selected stretch.

2. STUDY AREA

In this study, the study area includes a stretch of the Euphrates River extended from Haditha dam to the city of Heet in Al-Anbar Governorate and the length of the stretch is estimated to be 124.4 km. Along the studied river stretch, there are several towns, villages, agricultural

farms, and developments. The developments include many illegal businesses that dispose of pollutants in the Euphrates River. In addition, many sewage outfalls are disposing of raw sewage into the Euphrates River. **Figs. 1** and **2** show the location of the study area. The coordinates of the selected stretch of the Euphrates River are (N 34 12 13.47) and (E 42 21 35.66) near Haditha dam while (N33 38 17.36) and (E 42 50 34.89) at the town of Heet near the location of the gauging station.

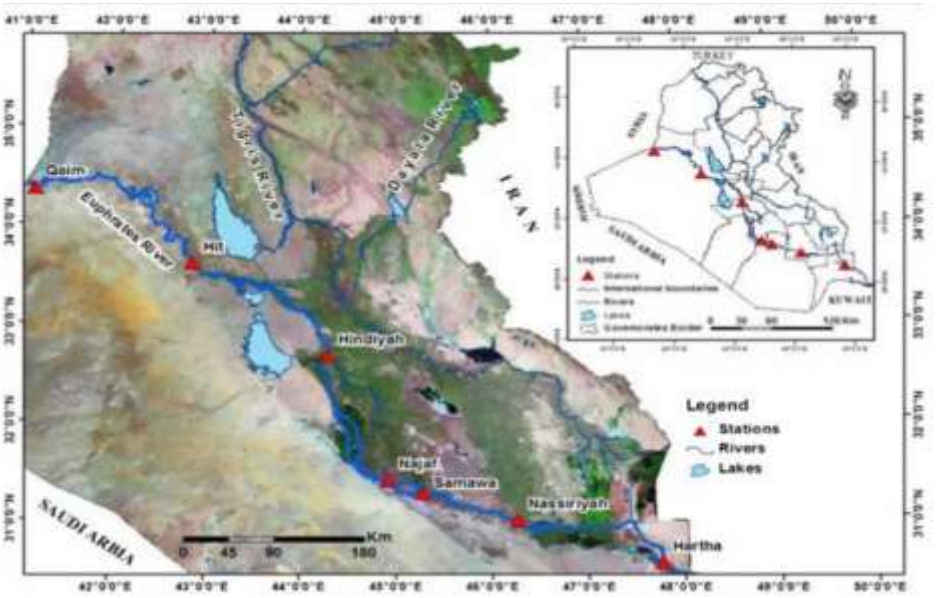

Figure 1. Euphrates River in Iraq

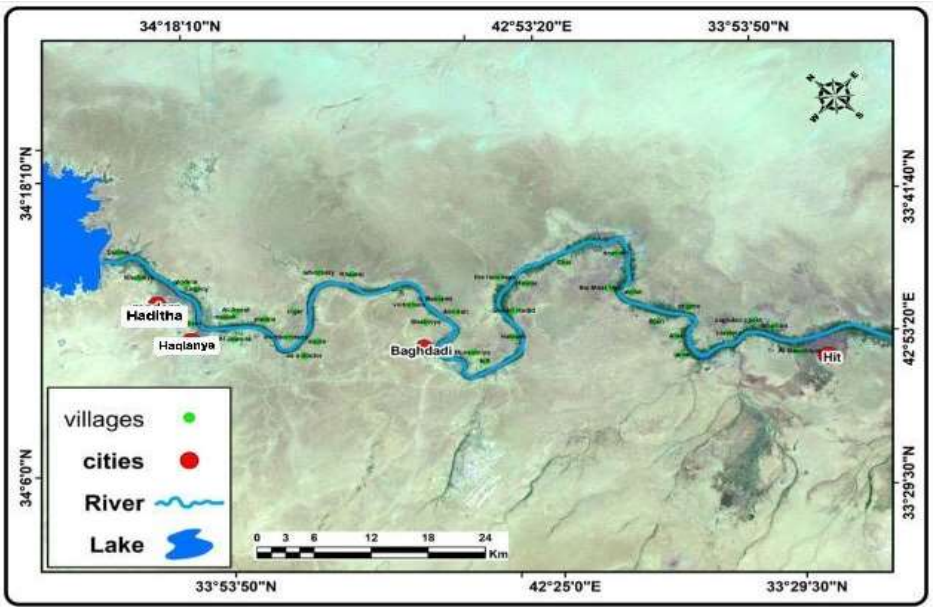

Figure 2. Location of study area between Haditha and Heet

3. GOVERNING EQUATIONS

The following equations represent the mathematical model for the river sediment analysis process using the iRIC software.

3. 1 Flow Equations

The flow equations mainly include both continuity and momentum equations in the *x* and y directions. The continuity equation is given as:

$$\frac{\partial h}{\partial t}+\frac{\partial (hu)}{\partial x}+\frac{\partial (hv)}{\partial y}=0 \tag{1}$$

The momentum equations in *x* directions are described by Eqs. (2 and 3).

$$\frac{\partial (uh)}{\partial t}+u\frac{\partial (uh)}{\partial x}+v\frac{\partial (vh)}{\partial y}-f(vh) = -gh\ \frac{\partial H}{\partial x}+2\frac{\partial}{\partial x}v_{xx}\frac{\partial (uh)}{\partial x}+\frac{\partial}{\partial y}v_{xy}\frac{\partial (uh)}{\partial y}+\frac{\partial}{\partial y}v_{xy}\frac{\partial (vh)}{\partial x}+\frac{\tau_s}{\rho}-\frac{\tau_{bx}}{\rho}-\frac{\tau_{tx}}{\rho} \tag{2}$$

$$\frac{\partial (vh)}{\partial t}+u\frac{\partial (vh)}{\partial x}+v\frac{\partial (vh)}{\partial y}+f(uh) = -gh\ \frac{\partial H}{\partial y}+\frac{\partial}{\partial x}v_{xy}\frac{\partial (vh)}{\partial x}+\frac{\partial}{\partial x}v_{xy}\frac{\partial (uh)}{\partial y}+2\frac{\partial}{\partial y}v_{yy}\frac{\partial (vh)}{\partial x}+\frac{\tau_s}{\rho}-\frac{\tau_{by}}{\rho}-\frac{\tau_{ty}}{\rho} \tag{3}$$

where

$$\frac{\tau_{bx}}{\rho}=C_f\,u\sqrt{u^2+v^2} \tag{4a}$$

$$\frac{\tau_{by}}{\rho}=C_f\,v\sqrt{u^2+v^2} \tag{4b}$$

$$\frac{\tau_{tx}}{\rho}=C_t\,u\sqrt{u^2+v^2} \tag{5a}$$

$$\frac{\tau_{ty}}{\rho}=C_t\,v\sqrt{u^2+v^2} \tag{5b}$$

$(h=N_i\,h_i);\ (u=N_i\,u_i);\quad (v=N_i\,v_{i)}$

where
t is time (s)
u, v are flow velocity components in x, y direction (m/s)
g is gravity acceleration (m/s^2)
h is depth (m)
H is water level (depth+ground elevation: h + z_0) (m)

f is Coriolis parameter
$v_{xx}, v_{xy}, v_{yx}, v_{yy}$ is kinematic eddy viscosity (m^2/s)
τ_{bx}, τ_{by} is bottom shear stress component of *x, y* direction ($kg/m.s^2$)
τ_{tx}, τ_{ty} is vegetation shear stress component of *x, y* direction ($kg/m.s^2$)
τ_s is shear stress on the water surface ($kg/m.s^2$)
C_f is the River bed friction coefficient
C_t is the coefficient of vegetation resistance
ρ is water density (kg/m^3)

3.2 Discretization of Basic Equations

The flow Eqs. (1) to (3) are discretized in space variables by using the Galerkin finite element method (a kind of weighted residual method). The definition is shown below, using a linear triangular prism element N_i as shape function **(Connor and Brebbia, 1976).**

$$N_i = a_i + b_i x + c_i y \tag{6}$$

$$a_i = (x_j y_k - x_k y_j) 2s \tag{7}$$

$$b_i = (y_j - y_k)/2s \tag{8}$$

$$c_i = (x_k - x_j)/2s \tag{9}$$

where i, j, k are the vertexes of triangular elements and s is the area of a triangle in i, j, k

By substituting the shape function defined in Eqs. (6) to (9) into Eqs. (1) to (3), multiply N_i as weight function, and integrate with the definition domain of weight function.

$$\frac{\partial h_j}{\partial t}\int_s N_i N_j \, ds + \int_s N_i \left(N_j u_j \frac{\partial N_k}{\partial x} h_k + \frac{\partial N_j}{\partial x} u_j N_k h_k \right) ds + \int_s N_i \left(N_j v_j \frac{\partial N_k}{\partial y} h_k + \frac{\partial N_j}{\partial y} v_j N_k h_k \right) ds = 0 \tag{10}$$

where,

$$i = i, j, k \quad j = i, j, k \quad k = i, j, k \quad l = i, j, k$$

l is the edge length of the triangle element
n_x, n_y: *x, y* are components of the unit normal vector which create the boundary of the triangular element
It is better to consider the boundaries only, to cancel all the terms including n_x, n_y inside triangular elements. In addition, each factor can be easily calculated by the formula as shown in Eqs. (11) and (12).

$$\int_s N_i^a N_j^b N_k^c \, ds = \frac{a!\ b!\ c!}{(a+b+c+2)!}\ 2s \tag{11}$$

$$\int_l N_i^a \, N_j^b \, dl = \frac{a! \; b!}{(a+b+1)!} \; 2l \qquad (12)$$

3.3 Calculation of Turbulence Field

Turbulence means disordered flow that contains eddies of various sizes and structures. In iRIC software Nacy 2DH, allows the user to select one of the three methods of computing turbulence, and these methods are a zero-equation model, k-ε model, and direct input kinematic eddy viscosity. The k-ε model is used for this purpose and it describes the eddy viscosity coefficient, v by:

$$v = C_\mu \; \frac{k}{\varepsilon} \qquad (13)$$

where,
C_μ: constant (0.09)
k : turbulent energy (m^2/s^2)
ε : energy dissipation rate (m^2/s^3)
According to the empirical equation of turbulent energy, k proposed by **(Nezu, et al., 1993)**

$$\frac{k}{u_*^2} = 4.78 \exp\left(-2 \; \frac{z}{h}\right) \qquad (14)$$

It can be evaluated by the following equation which can be calculated by water depth integration.

$$k = 2.07 \; u_*^2 \qquad (15)$$

Energy dissipation rate ε can be evaluated as:

$$\varepsilon = C_e \frac{k^{3/2}}{l} \qquad (16)$$

C_e is a constant of (0.17)

Thus, the kinematic eddy viscosity v can be calculated without solving the transport equation of energy dissipation rate ε and turbulent energy k. The kinematic eddy viscosity v is a kind of apparent kinematic viscosity coefficient in turbulence. The values of ν_{xx} , ν_{xy} , ν_{yy} in Eqs. (1) and (3) are directly specified if kinematic eddy viscosity is directly input. It is also possible to change each element (cell) in a specified space.

3.4 Calculation of Bottom Friction

In Nacys 2DH iRIC, the bottom friction can be set using Manning's roughness coefficient n. The following equation expresses the river bed friction coefficient in Eq. (4).

$$C_f = \frac{g \; n^2}{h^{1/3}} \qquad (17)$$

Manning's coefficient of roughness, n is possible to be changed in the space as specified by each element (cell).

3.5 Sediment Transport Equation

In iRIC Nacy 2DH two types of sediment can be selected to calculate riverbed variation: (i) is bed load only, and (ii) is the bed with suspended sediment load. Moreover, uniform grain diameter and mixed grain diameter can be selected as riverbed material. The dimensionless shear stress is defined by the following equation, by non-dimensional riverbed shear stress which is used in the calculation of sediment discharge.

$$\tau_* = \frac{u_*^2}{s\ g\ d} \tag{18}$$

u_*: bottom friction velocity (m/s)
s : submerged specific gravity of sediment
d : grain diameter of river bed material (m)

The total bedload, q_b of depth-averaged flow, velocity is calculated by **(Meyer-Peter and Müller, 1948).**

$$q_b = 8\sqrt{\left(\frac{\sigma}{\rho} - 1\right)\ g\ d^3}\ \ (\tau_*' - \tau_{*c})^{1.5} \tag{19}$$

d : grain diameter (m)
σ : gravel density (kg/m^3)
τ_{*c} : Critical tractive force **(Iwagaki, 1956)**
τ_*' : Calculated by using Eq. (14)

$$\frac{\bar{U}}{u_*} = \begin{cases} 7.66\ \left(\frac{h}{2d}\right)^{1/6}\ \left(\frac{\tau_*'}{\tau_*}\right)^{2/3} & \frac{h}{2d} < 500\ \ 11.59 \\ \left(\frac{h}{2d}\right)^{1/10}\ \left(\frac{\tau_*'}{\tau_*}\right)^{3/5} & \frac{h}{2d} \geq 500 \end{cases} \tag{20}$$

$\bar{U}$: Vertical average flow velocity in the flow direction
Total sediment discharge converts to the normal (n) and tangential directions (s) of streamlining, considering the effect of secondary flow and riverbed slope due to streamlining curvature of depth-averaged flow velocity **(Nakajima et al., 2001; Hasegawa, 1985).**

$$q_s = q_b\left(\frac{v_b}{V_b} - \sqrt{\frac{\tau_{*c}}{\mu_s\ \mu_k\ \tau_*}}\ \frac{\partial z}{\partial s}\right) \tag{21}$$

$$q_n = q_b\left(\frac{u_b}{V_b} - \sqrt{\frac{\tau_{*c}}{\mu_s\ \mu_k\ \tau_*}}\ \frac{\partial z}{\partial n}\right) \tag{22}$$

where
q_s is (s) direction component of sediment discharge near a riverbed V_b (kg/s)
q_n is (n) direction component of sediment discharge near a riverbed V_b (kg/s)

V_b is the absolute value of velocity near the riverbed (m/s)
v_b is (s) direction component of flow velocity near the riverbed V_b (m/s)
u_b is (n) direction component of flow velocity near the riverbed V_b (m/s)
μ_s is the static friction factor
μ_k is the kinetic friction factor
z is the height of the riverbed (m)

3.6 Calculation of Flow Velocity near the Riverbed

The flow velocity near the river bed is calculated by the streamlined curvature of a depth-averaged flow velocity as below.

$$v_b = 5.8\ u_* \qquad u_b = -N\ \frac{h}{r}\ v_b \tag{23}$$

$$\frac{1}{r} = \frac{1}{(u^2+v^2)^{3/2}} \left\{ u\left(u\frac{\partial v}{\partial x} - v\frac{\partial u}{\partial x}\right) + v\left(u\frac{\partial v}{\partial y} - v\frac{\partial u}{\partial y}\right)\right\} \tag{24}$$

N is constant = 7, Engelund **(Engelund, 1974)**
r is the curvature radius of streamline (rad)
The velocity of buoyancy of suspended sediment, E_s is calculated as **(Itakura and Kishi, 1980; Kishi, 1973)**

$$E_s = K\left(\alpha_*\ \frac{1}{\tau_*}\ \frac{\rho}{\sigma}\ \frac{u_*}{w_0}\ \Omega - 1.0\right) \tag{25}$$

$$\Omega = 14.0\ \tau_* - 0.9$$

K is constant (0.008)
α_* is constant (0.14)
w_0 is sedimentation speed (calculated by the Rubey formula)**(Hubbert and Rubey, 1959)**.
Suspended sediment concentration at the referential level is calculated by the Rouse formula, **(von Bergen, et al., 1937)**:

$$\frac{C}{C_a} = \left(\frac{h-z}{z} - \frac{z_a}{h-z_a}\right)^z \tag{26}$$

$$z = \frac{w_0}{k\ u_*} \tag{27}$$

k is von Kármán coefficient
C is the concentration of suspended sediment at z
z_a is referential height (= 0.05 h)
The mass conservation equation for the depth-averaged concentration of suspended sediment is given as:

$$\frac{\partial(\bar{c}h)}{\partial t} + u\frac{\partial(\bar{c}h)}{\partial x} + v\frac{\partial(\bar{c}h)}{\partial y} = (E_s - C_a)w_0 + \frac{\partial}{\partial x}D_x\frac{\partial(\bar{c}h)}{\partial x} + \frac{\partial}{\partial y}D_y\frac{\partial(\bar{c}h)}{\partial y} \tag{28}$$

D_x, D_y is diffusion coefficient of suspended sediment
Eq. (28) is the same as the basic equation of flow; it discretizes the spatial variables by Galerkin finite element which is a kind of weighted residual method.
The continuity equation of sediment transport in horizontal two-dimension is:

$$\frac{\partial z}{\partial t} + \frac{1}{1-\lambda}\left\{\frac{\partial q_x}{\partial x} + \frac{\partial q_y}{\partial x} - (E_s - C_a)w_0\right\} = 0 \quad (29)$$

$$q_x = q_n \cos\theta - q_s \sin\theta \quad (30)$$

$$q_y = q_n \sin\theta + q_s \cos\theta \quad (31)$$

$$\theta = tan^{-1}(\bar{v}/\bar{u}) \quad (32)$$

$\bar{u}$, $\bar{v}$ are (x, y) direction components of depth-averaged flow velocity

In the case to calculate bed load only, the hoisting speed of suspended sediment Es and benchmark concentration C_a is zero.
When non-uniform grain diameter is selected for the riverbed material, the basic equations to be used for riverbed deformation are described below. A non-uniform grain-size riverbed is made up of a certain grading of riverbed material. To handle this grading mathematically, the cumulative grading curve is divided into n layers as shown in **Fig. 1**, and each layer is expressed by its representative grain size d_k and the probability of that grain size existing P_k. Median diameter d_m is defined by:

$$d_m = \sum_{k=1}^{n} P_k \, d_k \quad (33)$$

where
d_k is the representative grain size of layer k,
P_k is the layer k's grain size as a proportion of the entire riverbed.

4. FIELDWORK

4.1 Sediment Sampling

For the studies stretch of the Euphrates River, the fieldwork included the collection of two types of samples from the river at three selected sections **(Fig. 3)**. The first type of sample was collected from the bed and banks of the river using a Van Veen grab SG sampler shown in **Fig. 4**. The sieve analysis was conducted and the grading curve was plotted where the median size of the bed material was determined from that curve. The type of alluvial material of the river is playing important role in forming the river geometry and morphology **(Church, 2006)**.
The river bed material samples were collected during the bathymetric survey from 3 locations along the studied river stretch, particularly from islands and meander existing in the Euphrates River. Details of the location of the samples are shown in **Table 1**. The second type of sample was water sampling.

Table 1. Number of considered water samples and bed material samples

Stations	No. Water Samples	No. Bed Material Samples	Coordinates
Station 1	7	5	34 11 06 N 42 32 03 E
Station 2	8	4	34 09 32 N 42 23 00 E
Station 3	8	7	34 07 56 N 42 23 02 E

Figure 3. Locations of the bed material samples along the study reach.

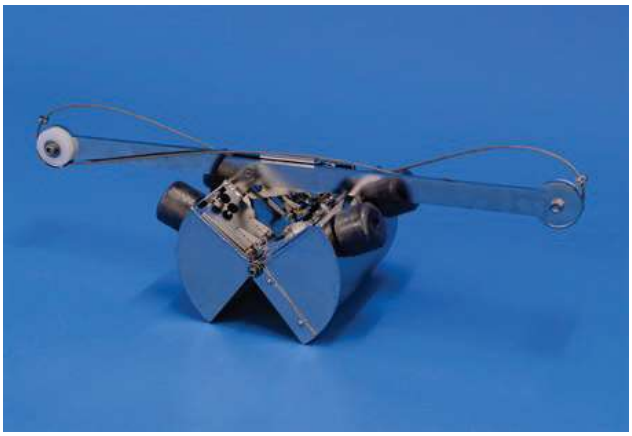

Figure 4. The Van Veen Grab is used for collecting bed material samples.

4.2 Water Sampling

Water samples were taken from the same river section used for sampling bed material as shown in **Figs. 3 and 5** show the water samples with their labels. Each label represents the samples taken from a certain river section of the Euphrates River.

5. THE SCENARIOS

To consider various flow conditions in the simulation, three different scenarios have been considered and details on these scenarios are described in the subsections shown below.

Figure 5. Water samples

5.1 First Scenario

The software was run using the lowest discharge of the Euphrates River at the selected stretch in the last 5 years which was equal to Q=172m^3/sec. As can be seen in **Fig. 6(a)**, the velocity was low since the discharge was the lowest recorded in the period of the historical record.

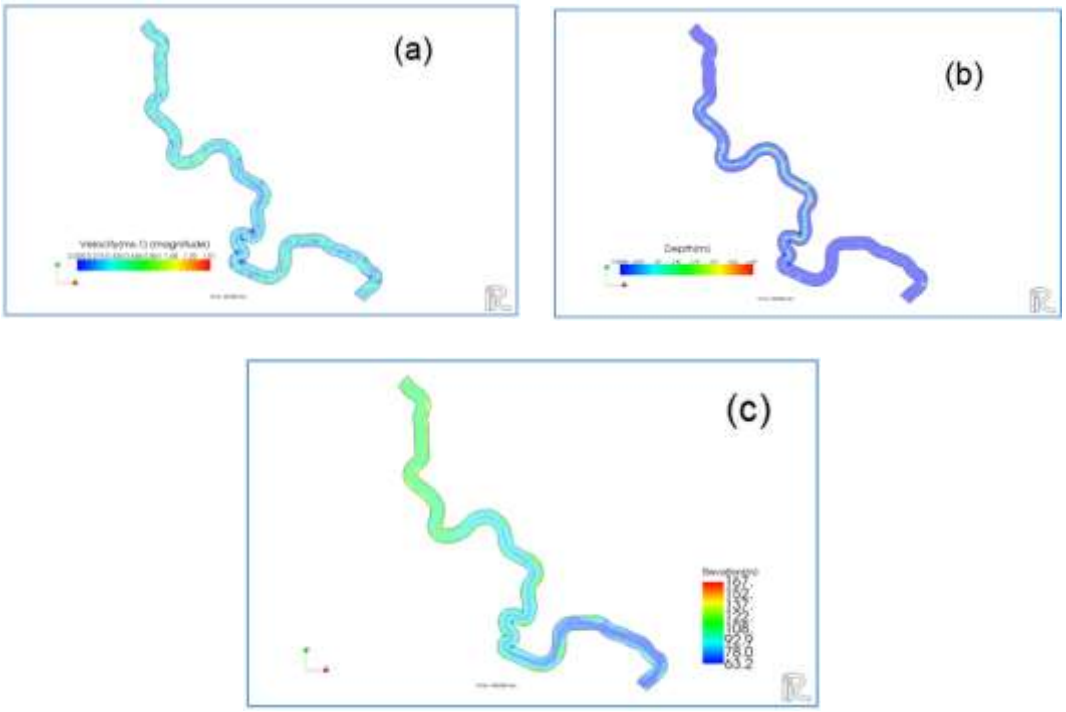

Figure 6. Simulation of velocity, elevation, and flow depth while minimal flow criteria in the first scenario. (a) velocity (b) river depth, and (c) for the elevation.

Fig. 6(b) shows the water depth for the studied river stretch of the Euphrates River for the first scenario. It can be noticed that the highest river depth was found near the convex locations of the river bends in addition to the middle of the section of the straight river stretch. The bed elevations along the studied Euphrates River stretch are shown in **Fig. 6(c).**

5.2 Second Scenario

The model was run using the average discharge for the last 5 years record which was equal to Q=400 m^3/sec. As can be seen in **Fig. 7(a),** the simulation results showed that the maximum velocity was 1.73 m/sec. It was also recognized that the maximum velocity was found at the river bends. **Fig.7(b)** shows that the maximum depth was 4.43 m. The minimum bed elevation was 62.4m in Heet. Due to high velocity, scour occurred and reduced the bed elevations. The bed elevations are shown in **Fig. 7(c)**.

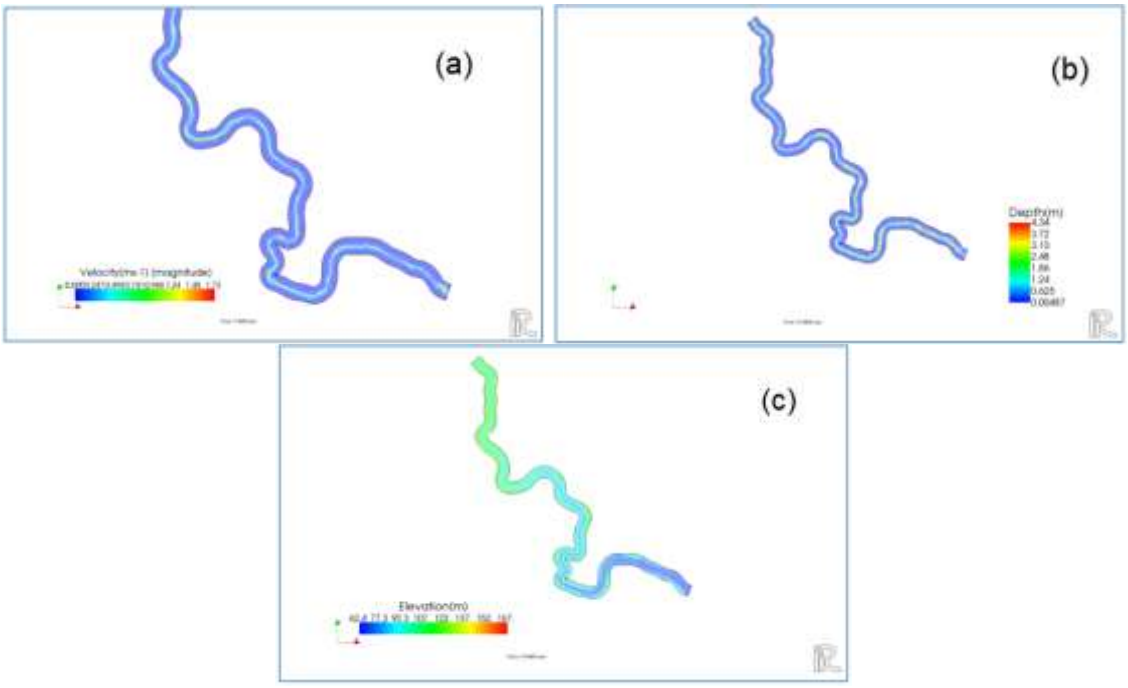

Figure 7. Simulation of velocity, elevation, and flow depth while minimal flow criteria in the second scenario. (a) velocity (b) river depth, and (c) for the elevation.

5.3 Third Scenario

The software was run using the maximum discharge recorded in the last 5 years which was equal to Q=1022 m^3/sec. **Fig. 8** shows the predicted velocities, water depth, and bed elevations for the studied stretch of the Euphrates River.

6. RESULTS AND ANALYSIS

The velocity and depth are used to check the model output. The details are given in **Tables 2 and 3**. The calibration was first conducted using the data collected from the Euphrates river in the city of Heet. The selected river section in Heet city has a sedimentation problem

and the collected data on sediment load and river bed can be used to predict the river condition in the future for both high and low flows. The velocity was measured using the M9 device. Several comparisons were conducted between the measured and simulation results.

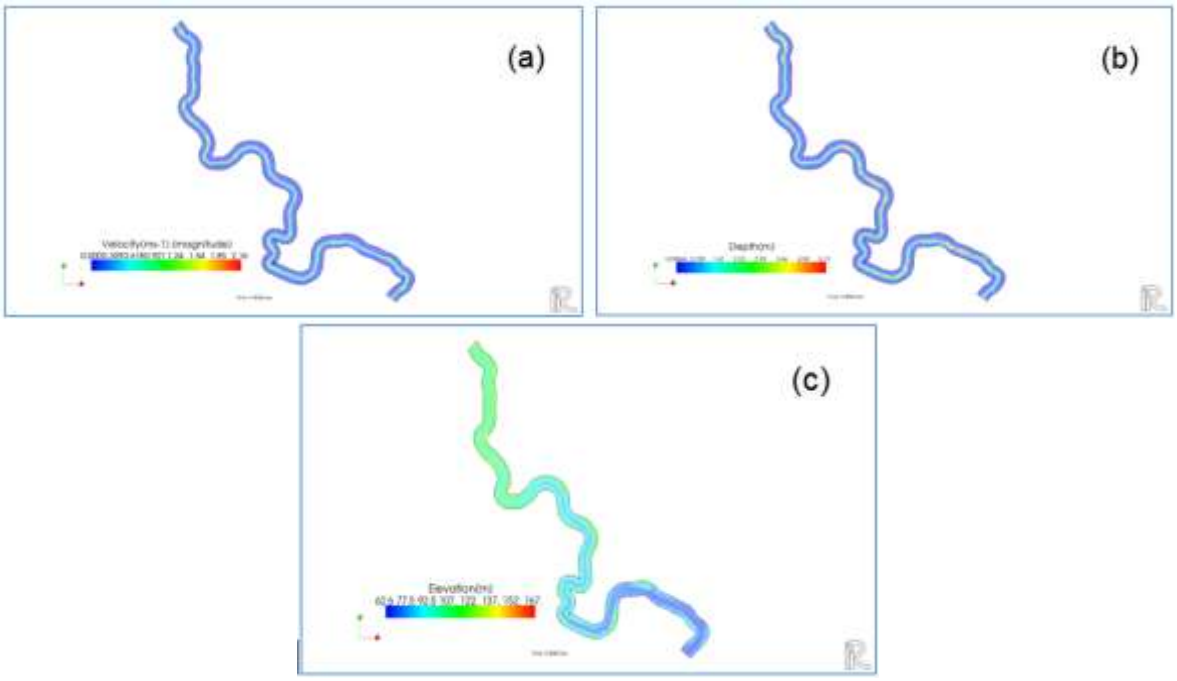

Figure 8. Simulation of velocity, elevation, and flow depth while minimal flow criteria in the third scenario. (a) velocity (b) river depth, and (c) is for elevation.

Table 2. Model accuracy assessment using data of measured average velocity

No.	Measured Average Velocity (m/s)	Simulated Average Velocity (m/s)	Absolute Error (m/s)	Square of the Error	Absolute Error Divided by Measured Average Velocity	statistical Indices	Value of the Statistical Index
1	0.357	0.48	0.123	0.015129	0.344	MAD	0.071818
2	0.442	0.58	0.138	0.019044	0.312	MSE	0.008213
3	0.192	0.121	0.071	0.005041	0.369	RMSE	0.090628
4	0.258	0.379	0.121	0.014641	0.468	MAPE	0.200999
5	0.305	0.407	0.102	0.010404	0.334		
6	0.644	0.525	0.119	0.014161	0.184		
7	0.593	0.455	0.138	0.019044	0.232		
8	0.333	0.43	0.097	0.009409	0.291		
9	0.301	0.404	0.103	0.010609	0.342		
10	0.385	0.505	0.12	0.0144	0.311		
11	0.216	0.105	0.111	0.012321	0.513		
sum	2.777	2.831	0.79	0.090348	2.210		

Four statistical indices were used to evaluate the model predictions and the measured average flow velocities were used to assess the model accuracy after the calibration process

was conducted. The values of the statistical indices such as Mean Absolute Deviation (MAD), Mean Square Error (MSE), Root MSE (RMSE), and Mean Absolute Percentage Error (MAPE) were calculated between measured velocities and predicted velocities and found to be 0.071818, 0.008213, 0.090628 and 0.200999 respectively. More details are given in **Table 2**. In general, MAPE provides values higher than the other indices and this is because it gave the difference between the predicted and measured values as a percentage.

Additionally, a graphical comparison between simulated and measured average velocities along the cross-section was drawn for model performance evaluation. The measured depths along a selected river section (in Heet city) are used to assess the model accuracy after the calibration process is conducted. The values of the statistical indexes such as Absolute Deviation (MAD), Mean Square Error (MSE), Root MSE (RMSE), and Mean Absolute Percentage Error (MAPE) are calculated between the measured velocities and the predicted depths are 0.113164, 0.029473, 0.171678, and 0.107696 respectively. More details are given in **Table 3.**

Table 3. Model accuracy assessment using data of measured average depth

No.	Measured Depth (m)	Simulated Depth (m)	Absolute Error (m)	Square of the Error	Absolute Error Divided by Measured Depth	statistical Indices	Value of the Statistical Index
1	0.54	0.38	0.16	0.0256	0.296	MAD	0.113164
2	0.53	0.42	0.11	0.0121	0.207	MSE	0.029473
3	1.31	1.063	0.247	0.061009	0.188	RMSE	0.171678
4	1.55	1.3896	0.1604	0.025728	0.103	MAPE	0.107696
5	1.36	1.66	0.3	0.09	0.220		
6	0.79	0.52	0.27	0.0729	0.341		
7	3.69	3.352	0.338	0.114244	0.091		
8	1.8	1.6892	0.1108	0.012277	0.061		
9	0.42	0.372	0.048	0.002025	0.107		
10	0.5	0.319	0.181	0.032761	0.362		
sum	8.56	7.9122	1.2448	0.419644	1.184		

7. CONCLUSIONS

In this study, the hydromorphodynamics of a selected stretch of the Euphrates River was simulated using the NACY 2DH model. The topographical and hydraulic data were used in the simulation process. The stretch included in the simulation was approximately 124.4 km and extended from Haditha dam to the city of Heet in Al-Anbar Governorate. Samples from selected sites along the river were taken and laboratory tests were conducted to determine the grading curve of the river bed and bank material. Input data such as river cross sections, median size (D_{50}) of the river material, and Manning coefficient of roughness (n) were used in the calibration process. The hydromorphodynamics of the Euphrates River were simulated for three possible scenarios. The scenarios were based on three different discharges (low, average, and flood discharge). The main conclusions derived from the present study are

1. The hydromorphodynamics of the Euphrates River (between Hadith Dam and the city of Heet) were successfully predicted. The simulation included flow conditions with low river discharge (Q=172 m^3/sec), average river discharge (400 m^3/sec), and flood river discharge (Q=1022 m^3/sec). The model calibration was conducted based on a recommended value of Manning roughness coefficient (n) of the Euphrates River which is equal to 0.033 and a value of median particle size (D_{50}) of 0.54mm.
2. The simulation results for the first and second scenarios (using low and average discharges) were validated using measured velocities and water depths at the section of the Euphrates River in the city of Heet. The simulated maximum velocity and water depth when Q=400 m^3/s was found to be 1.73 m/s and 4.45 m respectively. The simulation confirmed that the previous values occurred in the straight and meandering portions of the Euphrates River.
3. The statistical indices used to check the predicted values of the velocities in various locations of the Euphrates River section at the city of Heet were Mean Absolute Deviation (MAD), Mean Square Error (MSE), Root MSE (RMSE), and The Mean Absolute Percentage Error (MAPE). For the first scenario, the values of MAD, MSE, RMSE, and MAPE were found to be 0.19, 0.046, 0.21, and 0.17 respectively while the values for the second scenario were found to be 0.07, 0.01, 0.01, and 0.13 respectively. The values of the statistical indices confirm the accuracy of the prediction of model iRIC Nacy2DH.
4. The same procedure was followed to double-check the model accuracy using data on water depth in a selected section. The results of model prediction were found also satisfactory.
5. After the model accuracy was checked, the worst scenario was simulated and, in this scenario, a flood discharge of 1022 m^3/s was considered. The main objective of the 2D simulation is to demonstrate the scouring and deposition areas in the river sections. In the absence of the data on such an extreme case, no validation can be made but the simulation results can be accepted since the model was validated before and was applied to simulate this extreme case.

REFERENCES

Attard, M. E., 2012. Evaluation of ADCPs for suspended sediment transport monitoring*, Fraser River, British Columbia* Environment: Department of Geography.

Church, M., 2006. Bed material transport and the morphology of alluvial river channels. *Annu. Rev. Earth Planet. Sci.*, 34, pp. 325-354. doi:10.1146/annurev.earth.33.092203.122721

Engelund, F., 1974. Flow and bed topography in channel bends. *Journal of the Hydraulics Division*, 100(11), pp. 1631-1648. doi: 10.1061/JYCEAJ.0004109

Gharbi, M., Soualmia, A., Dartus, D., Masbernat, L., 2014a. A comparative analysis of Lajeunesse model with other used bed load models - effects on river morphological changes, *Journal of Water Resources and Ocean Science*, 3(5), pp. 61–68. doi: 10.11648/j.wros.20140305.12

Goniva, G., Gruber, K., Koss, C., 2012. *Sediment erosion a numerical and experimental study*. Taylor and Francis, London, UK.

Hasegawa, A., 1985. Self-organization processes in continuous media. *Advances in physics*, *34*(1), pp. 1-42. doi:10.1080/00018738500101721

Hiroshi, T., Hajime, N., Kenji, K., Yasuyuki, B., Hao, Z., 2011. Effects of hydraulic structures on river morphological processes. *International Journal of Sediment Research*, 26 (3), pp. 283-303. doi:10.1016/S1001-6279(11)60094-2

Hubbert, M. K., Rubey, W. W., 1959. Role of fluid pressure in mechanics of overthrust faultingi. mechanics of fluid-filled porous solids and its application to overthrust faulting. *GSA Bulletin*, 70(2), pp. 115-166. doi:10.1130/0016-7606(1959)70[115:ROFPIM]2.0.CO;2

Hydar, L. A., Badronnisa, Y., Thamer, A. M., Yasuyuki, S., Mohd Shahrizal A., Balqis, M., 2019. Improving the hydro-morpho dynamics of a river confluence by using vanes, *Resources*, 8(9), pp. 1-22.

Itakura, T., Kishi, T., 1980. Open channel flow with suspended sediments. *Journal of the Hydraulics Division*, 106(8), pp. 1325-1343. doi:10.1061/JYCEAJ.0005483

Iwagaki, Y., 1956. (I) Hydrodynamical study on critical tractive force. *Transactions of the Japan Society of Civil Engineers*, 41(1956), pp. 1-21. doi:10.2208/jscej1949.1956.41_1

Kamel, A., 2008. Application of a hydrodynamic MIKE 11 model for the Euphrates River in Iraq. *Slovak Journal of Civil Engineering*, 2(1), pp. 1-7.

Khudair, B.H., 2019. Influent flow rate effect on sewage pump station performance based on organic and sediment loading. *Journal of Engineering*, 25(9), pp. 1-11. doi: 10.31026/j.eng.2019.09.1.

Kishi, T.; Kuroki, M., 1973. Bed Forms and resistance to flow in erodible-bed channels. *Bull. Fac. Eng. Hokkaido Univ.*, *67*, pp. 1–23.

Meyer-Peter, E.; Müller, R., 1948. Formulas for bed-load transport. In Proceedings of the 2nd Meeting of the International Association for Hydraulic Structures Research, Delft, The Netherlands, 2, pp. 39–64.

Mingfu, G., Qiuhua, L., 2017. A two-dimensional hydro-morphological model for river hydraulics and morphology with vegetation. *Environmental Modelling & Software,* 88(2), pp. 10-21. doi:10.1016/j.envsoft.2016.11.008

Mustafa, A.S., Sulaiman, S.O., and Hussein, O.M., 2016. Application of swat model for sediment loads from valleys transmitted to Haditha reservoir. *Journal of Engineering*, 22(1), pp. 184-197.

Nakajima, A., Hashimoto, K., Watanabe, T., 2001. Recent studies on super-hydrophobic films. *Molecular Materials and Functional Polymers*, pp. 31-41. doi:10.1007/s007060170142

Nezu, I., Tominaga, A., and Nakagawa, H., 1993. Field measurements of secondary currents in straight rivers. *Journal of Hydraulic Engineering*, 119(5), pp. 598-614. doi:10.1061/(ASCE)0733-9429(1993)119:5(598)

Von Rergen, H., Howland, W., Lenz, A. T., Stevens, J., Mavis, F., Rouse, H., and White, M. P., 1937. Discussion on Open Channels of adverse slope. *Transactions of the American Society of Civil Engineers*, 102(1), pp. 661-676. doi:10.1061/TACEAT.0004888